APPLIED AND ENVIRONMENTAL MICROBIOLOGY, Dec. 2002, p. 6310–6320 Vol. 68, No. 12
0099-2240/02/$04.00+0 DOI: 10.1128/AEM.68.12.6310–6320.2002
Copyright © 2002, American Society for Microbiology. All Rights Reserved.

Conspicuous Veils Formed by Vibrioid Bacteria on Sulfidic Marine Sediment

Roland Thar* and Michael Kühl

Marine Biological Laboratory, University of Copenhagen, 3000 Helsingør, Denmark

Received 28 June 2002/Accepted 5 September 2002

We describe the morphology and behavior of a hitherto unknown bacterial species that forms conspicuous veils (typical dimensions, 30 by 30 mm) on sulfidic marine sediment. The new bacteria were enriched on complex sulfidic medium within a benthic gradient chamber in oxygen-sulfide countergradients, but the bacteria have so far not been isolated in pure culture, and a detailed characterization of their metabolism is still lacking. The bacteria are colorless, gram-negative, and vibrioid-shaped (1.3- to 2.5- by 4- to 10-μm) cells that multiply by binary division and contain several spherical inclusions of poly-β-hydroxybutyric acid. The cells have bipolar polytrichous flagella and exhibit a unique swimming pattern, rotating and translating along their short axis. Free-swimming cells showed aerotaxis and aggregated at ca. 2 μM oxygen within opposing oxygen-sulfide gradients, where they were able to attach via a mucous stalk, forming a cohesive whitish veil at the oxic-anoxic interface. Bacteria attached to the veil kept rotating and adapted their stalk lengths dynamically to changing oxygen concentrations. The joint action of rotating bacteria on the veil induced a homogeneous water flow from the oxic water region toward the veil, whereby the oxygen uptake rate could be enhanced up to six times, as shown by model calculations. The veils showed a pronounced succession pattern. New veils were generated de novo within 24 h and had a homogeneous whitish translucent appearance. Bacterial competitors or eukaryotic predators were apparently kept away by the low oxygen concentration prevailing at the veil surface. Frequently, within 2 days the veil developed a honeycomb pattern of regularly spaced holes. After 4 days, most veils were colonized by grazing ciliates, leading to the fast disappearance of the new bacteria. Several-week-old veils finally developed into microbial mats consisting of green, purple, and colorless sulfur bacteria.

Marine sediments and biofilms are characterized by opposing gradients of chemical compounds, which can react with each other via exergonic redox reactions (6, 14). The best-investigated gradient systems are sulfide-oxygen or sulfide-nitrate countergradients, and a variety of microorganisms which are specialized in efficiently utilizing the energy released by the redox reaction of the two gradient compounds have been described. Detailed physiological studies of species which can be cultured in homogeneous media, e.g., *Thiobacillus* spp., have been performed (18). However, many conspicuous gradient microorganisms in natural habitats (e.g., the colorless sulfide oxidizer *Thiovulum majus*) can be kept in the laboratory only as enrichment cultures, and only a few species have been successfully isolated in pure culture based on gradient media (24). While detailed physiological studies are still lacking, the behavior and motility of gradient microorganisms, especially of the relatively large and easily identifiable colorless and photosynthetic sulfur-oxidizing bacteria, have been described in the literature for >100 years. Several ecological strategies have been described which can be classified based on the shapes and relative positions of the opposing gradients in time and space.

In the case of nonoverlapping gradients, the microorganisms must be able to store at least one redox compound intracellularly. Filamentous *Thioploca* spp. are able to concentrate large amounts of nitrate in their vacuoles by stretching out from the sediment surface into nitrate-containing water. Subsequently, they glide within their mucus sheets several centimeters down toward sulfidic sediment layers, where the stored nitrate is reduced by sulfide (16, 30). The giant bacterium *Thiomargarita namibiensis* is occasionally exposed to nitrate-rich water during periods of sediment resuspension, when it is able to refill its large nitrate vacuole. After sedimentation, *T. namibiensis* can survive for several months buried in nitrate-depleted sulfidic sediment by oxidizing ambient sulfide with its stored nitrate (29, 30).

If the chemical gradients overlap, microorganisms have simultaneous access to both chemical compounds. In the case of opposing oxygen-sulfide gradients, the bacteria outcompete the spontaneous chemical oxidation of sulfide. They aggregate in a thin layer at the oxic-anoxic interface, where their high substrate affinity and turnover can keep the concentration of dissolved oxygen and sulfide low, thereby reducing the depth interval where the opposing gradients overlap to a few hundred micrometers (13). Typical examples of such microorganisms are the chemolithotrophic sulfide-oxidizing *Beggiatoa* spp. (23) and *T. majus* (20), but the phototrophic purple sulfur bacterium *Marichromatium gracile* has also been shown to aggregate in a thin layer at the oxic-anoxic interface under conditions of darkness (33). The filamentous *Beggiatoa* spp. are restricted by their gliding motility to solid surfaces, where they can position themselves by phobic responses toward excessive oxygen or sulfide concentrations (17, 21, 25). The flagellated *Thiovulum* cells are able to aggregate by true chemotaxis (32) at their

* Corresponding author. Mailing address: Marine Biological Laboratory, University of Copenhagen, Strandpromenaden 5, 3000 Helsingør, Denmark. Phone: 45 49 21 33 44. Fax: 45 49 26 11 65. E-mail: rthar@zi.ku.dk.

preferred oxygen concentration above the sediment surface, where they are able to attach by a mucous stalk. Aggregations of attached *Thiovulum* cells form characteristic veils at the oxic-anoxic interface (7, 17).

A variety of motile gradient microorganisms can be found in sulfureta (i.e., marine benthos dominated by the sulfur cycle), which exhibit steep gradients of chemical (e.g., O_2, pH, and H_2S) and physical (e.g., light and temperature) variables. A typical sulfuretum is found at Nivå Bay (Denmark), extending over an area of ca. 250 m^2 with a maximal water depth of 1 m. Winter storms bury large amounts of decaying algae in the sediment. During summer, the buried organic substrate is utilized by sulfate-reducing bacteria, giving rise to high sulfide levels in the sediment. If calm weather prevails, the whole water body becomes anoxic, accompanied by massive development of purple sulfur bacteria. The complex microbial ecosystem found in Nivå Bay has been the subject of extensive studies (2, 6, 8, 9). During field work in the summer of 1999, we observed conspicuous whitish translucent veils above the sediment surface in Nivå Bay (Fig. 1A). Closer examination revealed that the veils were formed by a hitherto unknown bacterial species. Here, we describe the morphology, swimming pattern, chemical microenvironment, and veil formation of this new bacterium.

MATERIALS AND METHODS

Sampling sites and enrichment culture. Sulfidic sediment mixed with decaying seagrass and macroalgae was sampled from the upper 50 mm of the sediment in Nivå Bay (30 km north of Copenhagen, Denmark), and petri dishes (250-mm diameter; 150 mm high) were filled with it. The petri dishes were placed into an aquarium filled with seawater from the sampling site (15 to 20‰ salinity; 20°C) and exposed to dim daylight by being placed near a window.

Sulfidic sediment densely inhabited by *Zostera marina* at Aggersund (Limfjorden, Denmark) was sampled at 1-m water depth. The seagrass was removed together with the sediment to a depth of 20 cm with a spade and was placed directly into an aquarium (1.0 by 0.6 m; 0.8 m high). Illumination was provided by five 20-W halogen bulbs 30 cm from the sediment surface in a 12 h dark-12 h light cycle.

In both cases, the seawater was continually flushed with air, causing advective water movement with a velocity of ~5 mm s^{-1} above the sediment surface.

Benthic gradient chamber. A beaker with a constricted neck (volume, 100 ml; opening diameter, 75 mm) was filled with complex enrichment medium consisting of 1% (wt/vol) yeast extract (L21; Oxoid Ltd.), 1% (wt/vol) Lab-Lemco powder (L29; Oxoid Ltd.), and 1% (wt/vol) tryptone (L42; Oxoid Ltd.) dissolved in filtered seawater (15‰ salinity) amended with neutralized Na_2S solution to a final concentration of 10 mM sulfide (Fig. 2). A fine nylon mesh was placed in the opening, supporting a 10-mm-thick layer of washed sand with 150- to 210-μm grain size (Sand of Fontainebleau; KEBO Lab, Alberdslund, Denmark). The sand surface was positioned ca. 10 mm below the upper rim of the opening. The beaker was placed into a petri dish (250-mm diameter; 150 mm high) filled with filtered seawater (15‰ salinity; 20°C) and permanently flushed with air. Advective water movements provided a relatively homogeneous water flow of ca. 5 mm s^{-1} above the opening of the beaker. The setup was left undisturbed for 1 h before samples of the bacterial veils were inoculated into the upper 3 mm of the washed sand.

TEM. For transmission electron microscopy (TEM) of whole bacteria (full-mount TEM), seawater samples containing the bacteria were mixed 1:1 with 37% formaldehyde in methanol. The fixed bacteria were transferred onto a TEM grid covered with support film and stained for 30 s with saturated uranyl acetate in 96% ethanol. For thin sectioning, the bacteria were fixed in 4% (vol/vol) glutaraldehyde in seawater, postfixed in 4% (wt/vol) OsO_4 in seawater, stepwise dehydrated with increasing ethanol concentrations, and stained with saturated uranyl acetate in 96% ethanol. The sample was embedded in Epon and sectioned in slices ca.100 nm thick with an LKB Ultramicrotome. TEM was performed on a Zeiss EM 900 electron microscope. The internal structure of the bacteria was investigated by transferring TEM photographs of successive bacterial thin sections to transparent plastic plates. The plates were piled up, yielding a three-dimensional impression of the intracellular organization.

Microsensor measurements. Dissolved-oxygen measurements were done with Clark-type O_2 microsensors with a guard cathode (27) connected to a picoammeter (Unisense A/S, Århus, Denmark). The microsensors had a tip diameter of 10 to 20 μm and <1 to 2% stirring sensitivity. A two-point calibration was performed from microsensor readings in seawater (15‰ salinity; 20°C) flushed with air and nitrogen, respectively.

Dissolved hydrogen sulfide was measured with amperometric H_2S microsensors (19) connected to a picoammeter (Unisense A/S). The electrodes had a tip diameter of 10 to 20 μm and <1 to 2% stirring sensitivity. Calibration was performed in a closed glass vessel filled with anoxic phosphate buffer (50 mM; pH 7.0; 20°C). Sulfide standard stock solution (10 mM) was added to the buffer in several consecutive steps up to a final sulfide concentration of 0.5 mM (corresponding to an [H_2S] of 0.25 mM at pH 7.0). The calibration points obtained were fitted by linear regression. The linear equation obtained by the fitting procedure was used for converting the microsensor signal to H_2S concentrations. The molarity of the standard stock solution was determined by the titrimetric method described by Fonselius (11).

The microsensors were mounted on a computer-controlled motorized (Oriel Inc., Stratford, Conn.) micromanipulator (Märzhäuser GmbH, Wetzlar, Germany). The measured signals were transferred to a computerized data acquisition system, which also controlled the micromanipulator (Unisense A/S). Oxygen and sulfide concentration profiles were acquired with a step size of 100 or 200 μm either within flat glass capillary preparations or directly within enrichment cultures.

Flat glass capillary preparations. Light microscopic observations were made of bacterial samples in flat glass capillaries (internal dimensions, 8 by 0.8 by 40 mm^3; VitroCom Inc., Mountain Lakes, N.J.). The openings of the capillaries were sealed with petroleum jelly (Vaseline; Cheseborough-Pond Inc., Greenwich, Conn.) in order to avoid evaporation, which would cause convective water movements in the capillary. Opposing oxygen-sulfide gradients were prepared by filling one half of the capillary with an agar plug prepared from filtered seawater amended with neutralized sulfide solution (2 to 5 mM H_2S), whereas the other half of the capillary was filled with samples from the enrichment culture. A detailed description of this technique can be found in Thar and Kühl (33).

In situ video microscopy and flow fields. Video sequences were acquired with a charge-coupled device camera (EHD GmbH, Damme, Germany) mounted on a compound microscope and connected to a digital video recorder (Sony Inc.). In situ video microscopy was performed by attaching a 10× water immersion microscope objective (Olympus Inc., Melville, N.Y.) via an optical tube 150 mm long (Linos GmbH, Göttingen, Germany) directly to the charge-coupled device camera. Dark-field illumination was applied by illuminating the samples with a collimated light beam from a halogen lamp incident perpendicular to the optical axis.

Flow fields were visualized by video microscopy of latex beads (diameter, 1 μm) added to the seawater in various microscope preparations. The movements of the latex beads were tracked and quantified by analyzing the video recordings frame by frame (time steps, 0.04 s). Only beads moving within the focal plane were taken into account.

RESULTS

Conspicuous whitish veils covering the surface of sulfidic sediment (mean grain size, 350 μm) at water depths of 0 to 0.5 m in Nivå Bay were observed from May to September in the years 1999 to 2001 (Fig. 1). The veils were mostly present in calm waters shortly after periods of windy weather. The wind action deposited decaying seagrass and macroalgae (mainly *Z. marina* and *Polysiphonia nigrescens*) on and within the sulfidic sediment upon which the veils subsequently developed. Upon microscopic examination of the veils, it was found that they were formed by a hitherto undescribed motile bacterium (Fig. 3).

Veil formation and species succession in laboratory enrichments. The fragile structure of the veils prohibited their undisturbed transport to our laboratory, but we succeeded in inducing veil formation in sediment samples incubated in the laboratory under a moderate advective flow of air-saturated

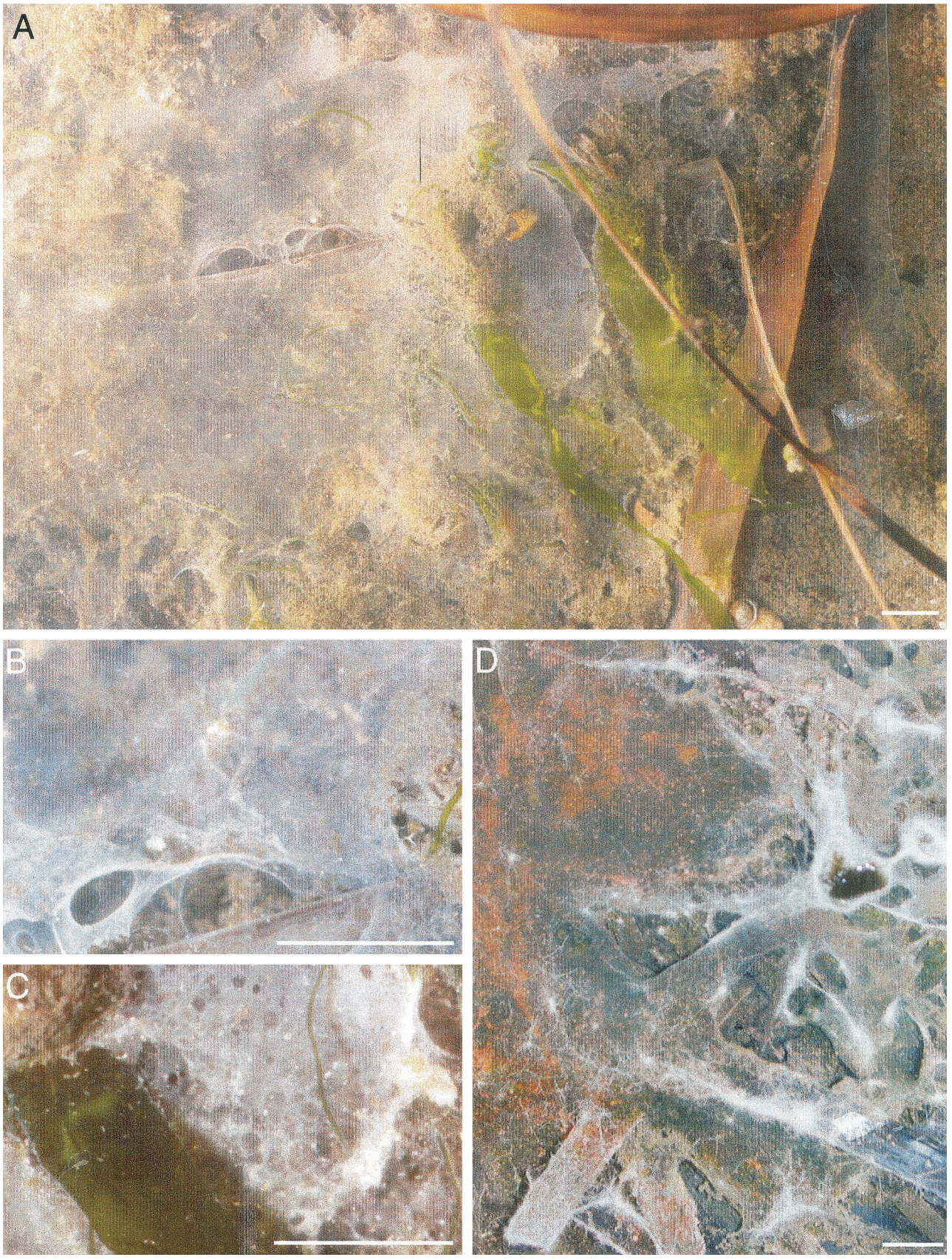

FIG. 1. Bacterial veils in enrichment cultures. (A) Whitish translucent veils covering sediment mixed with decaying seagrass and macroalgae. (B) Homogeneous veil region (detail of panel A). (C) Region showing holes in the veils (detail of panel A). (D) Bacterial mat of green, purple, and colorless sulfur bacteria formed at the former veil position after 4 weeks of incubation with 12-h–12-h dark-light illumination. Bars, 5 mm.

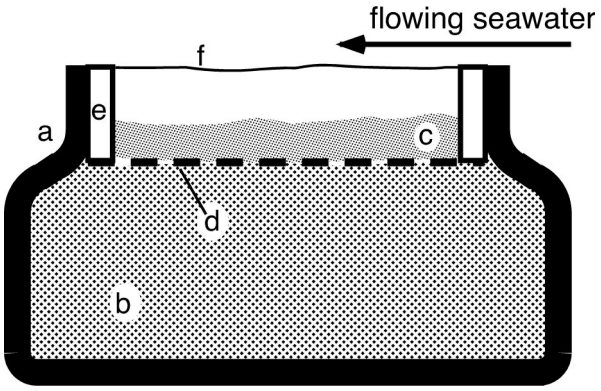

FIG. 2. Cross-section of benthic gradient chamber used for laboratory enrichment of veil-forming bacteria. a, beaker with constricted neck; b, liquid sulfidic medium; c, washed sand; d, nylon mesh attached to plastic ring (e); f, bacterial veil.

water mimicking the in situ conditions. After 1 to 3 days, the veils reappeared and often covered most of the sediment surface (Fig. 1A). Such newly formed veils showed a homogeneous whitish translucent appearance with typical extents of 30 by 30 mm (Fig. 1B). Typical distances between the veils and the sediment surface were 0 to 10 mm. The veils spanned depressions in the sediment surface or were attached to decaying algae. Only a few ciliates were observed on the veils. Frequently, the incubated sediment also contained veils formed by the sulfide-oxidizing bacterium *Thiovulum*, which were easily distinguished by the characteristic cell morphology and the spatial patterns formed by attached *Thiovulum* cells. Occasionally, the whitish translucent veils were overgrown by *Thiovulum* veils, with typical distances of 1 to 2 mm between the two veils.

A succession in the veil development could be observed if the enrichment culture was left undisturbed for several days. After 1 to 3 days, the veils became thicker, less translucent, and more nonhomogeneous. Frequently, the veils developed a regular pattern of holes with diameters of 400 ± 180 μm (mean ± standard deviation; $n = 10$), giving the veil a honeycomb-like appearance (Fig. 1C; see also Fig. 7A). After ~1 week, the veils were overgrown by filamentous *Beggiatoa* spp., and a dense ciliate population grazed away most of the vibrioid-shaped bacteria that formed the veils. After 4 weeks, the veils were replaced by a phototrophic bacterial mat, provided that the sediment was illuminated by an incandescent bulb (60 W; 0.4-m distance) during incubation. Green sulfur bacteria forming a homogeneous layer at the former position of the veils were covered by colonies of purple sulfur bacteria, *Beggiatoa* spp., filamentous cyanobacteria, and benthic ciliates (Fig. 1D). In order to keep the original veils for a longer period in the laboratory, the succession pattern was interrupted by mixing the upper 2 cm of the sediment every 3 to 7 days. New veils were generated de novo typically within 1 day. This method allowed us to keep the veils for ca. 4 weeks in enrichment culture.

We also observed the same types of veils and bacteria on sulfidic sediment samples from Aggersund, which were densely colonized by *Z. marina*. Three days after the sediments were sampled, the whitish translucent veils appeared in the enrichment culture on top of the sediment surface between the *Zostera* plants.

Morphology and motility. Light microscopy of the whitish translucent veils showed that they were predominantly composed of colorless vibrioid-shaped bacteria with dimensions of 1.3 to 2.5 by 4 to 10 μm (Fig. 3A). These bacteria, however, could not be detected in veils >1 week old. The cells multiplied by binary fission and showed up to five spherical refractive inclusions of up to 1-μm diameter (Fig. 3B and E). Sudan Black staining showed that the cell inclusions contained poly-β-hydroxybutyric acid (PHB). Cells inspected by full-mount TEM showed a bipolar polytrichous flagellation with flagella 6 to 8 μm in length (Fig. 3C and D). Occasionally, 300-nm-thick threads could be observed which appeared to be coiled up in a helix and consisted of <50-nm-thick filaments (Fig. 3D). Bacteria positioned next to such threads showed protrusions (50 to 100 nm in diameter; 50 to 300 nm in length) regularly spaced on the outer cell wall. TEM of thin sections showed a cell wall structure typical of gram-negative bacteria (Fig. 3G). Besides the PHB inclusions, two other structural elements could be observed inside the cell plasma. The cell wall was covered internally by spherical vesicles (~70 nm in diameter) (Fig. 3F). Furthermore, a three-layered structure was located below the cell wall at the polar ends of the cell (Fig. 3F to H). It consisted of three osmiophilic lines lying parallel to each other with a typical length of ca. 400 nm and a distance between the two outer, thicker lines of ca. 40 nm. The thickness of this structure was <100 nm (the resolution limit of thin sectioning). An additional ca. 50-nm-thick osmiophilic region was observed between the three-layered structure and the cell wall.

The bacteria showed a unique motility behavior, as they were permanently rotating around their short axes at a rate of 3.1 ± 0.8 rotations s^{-1} (mean ± standard deviation; $n = 10$). Reversals of the rotation direction were not observed. Free-swimming cells translated along the rotation axis with speeds of 74.9 ± 10.8 μm s^{-1} (mean ± standard deviation; $n = 10$), the convex side of the curved cell shape always in front. Thus, the polar ends of the bacteria described a path resembling a double helix with a pitch of 24.9 ± 4.2 μm (mean ± standard deviation; $n = 10$) (Fig. 4A and 5A). The bacteria were able to attach to particles or glass walls with a mucous stalk, which could not be visualized by light microscopy (Fig. 4B). Attached bacteria kept rotating along their short axes.

Observations in flat glass capillaries. The bacteria showed pronounced chemotactic behavior, which allowed them to accumulate in microoxic regions. They formed narrow bands 50 to 200 μm thick around sulfidic debris particles added to microscopy preparations within flat glass capillaries. Frequently, other free-swimming bacterial species (predominantly spirilla and cocci) could be observed within the bands. Microsensor measurements revealed that the bands were positioned at the oxic-anoxic interface within opposing oxygen-sulfide gradients (Fig. 6A). The borders of the bands toward the oxic region were always positioned at an oxygen concentration of ca. 2 μM. The bacteria within the band were all attached by their stalks, kept rotating, and pointed toward the oxic side. Particle tracking showed that the joint activity of the rotating bacteria created a water flow perpendicular to the bacterial band (Fig. 5B). The flow was always directed from the oxic toward the anoxic region, with typical flow velocities of 25.4 ± 8.0 μm s^{-1} (mean

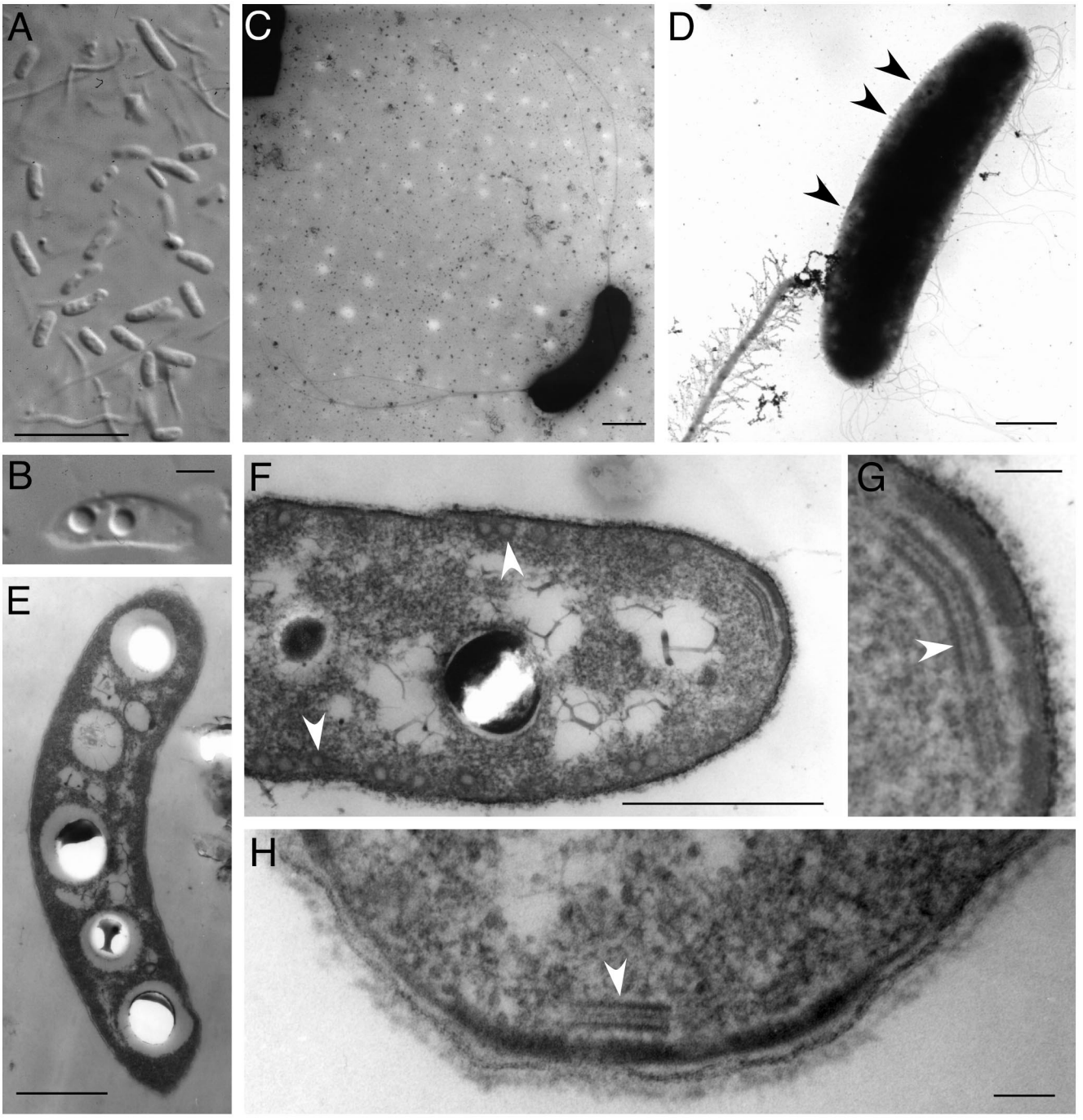

FIG. 3. Morphology of the new veil-forming bacteria. (A and B) Vibrioid-shaped bacteria showing PHB inclusions (Normarsky microscopy). (C) Bipolar polytrichous flagellation (full-mount TEM). (D) Bacterium with flagella next to possible remnant of bacterial stalk (full-mount TEM). Arrowheads indicate protrusions on the cell surface. (E) Bacterium with several PHB inclusions. (F) Spherical vesicles (arrowheads) positioned below the cell wall. (G and H) Three-layered osmiophilic structure (arrowheads) below polar ends of the cell wall. (E to H, TEM on thin-sectioned samples.) Bars, 10μm (A), 1μm (B to F), and 100 nm (G and H).

± standard deviation; $n = 13$). The necessary countercurrent occurred in regions where no bands were formed.

The formation of bacterial bands was also observed when samples of the veil were transferred into gradient capillaries. The sulfidic agar plugs in the capillaries sustained an opposing oxygen-sulfide gradient for ca. 24 h. During this period, all bacteria within the band kept rotating. After ~1 h, a whitish cohesive mucous web was observed at the anoxic side of the bacterial band. The rotating bacteria were apparently attached to this web. Bacteria trapped by debris particles in either anoxic or oxic regions (>20 μM O_2) showed decreasing swimming and rotational velocities and became immotile within 30

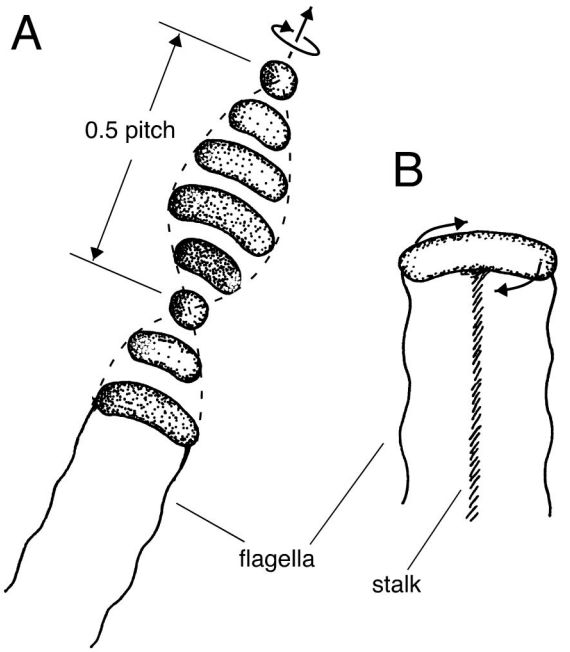

FIG. 4. Schematic drawings showing motility behavior of the bacterium. (A) Consecutive positions of a free-swimming cell; the swimming direction is indicated by an arrow. The flagella of the bacterium are indicated only at the first position. The polar ends of the cell describe a path resembling a double helix (broken lines). (B) Bacterium attached via a stalk. The rotational movement of the cell is indicated by the arrows.

min. Such immotile bacteria were never observed to regain motility, even if they were again exposed to microoxic conditions.

In situ observations of bacteria on veils. In situ video microscopy of veils in the enrichment culture showed that the bacteria were evenly distributed on the oxic side of the whitish translucent veils (Fig. 5C and D) ($t = 0$ s). Typical distances between neighboring bacteria were 10 to 20 μm. The bacteria were attached to the veils via stalks not exceeding 20 μm in length. They showed the same rotational movement observed in the bacterial bands formed in glass capillaries. The advective water flow was always parallel to the veil surface (Fig. 5D) ($t = 200$ s). The flow ceased when the aeration of the seawater was stopped for 80 s. The bacteria responded to this environmental change by increasing their stalk lengths. Within 80 s, the stalks gained ca. 100 μm (Fig. 5D) ($t = 0$ to 80 s). A net movement of the overlying water toward the veil was observed in this situation (Fig. 5D) ($t = 80$ s). The flow, with a velocity of 36.4 ± 9.3 μm s^{-1} (mean ± standard deviation; $n = 7$), was apparently induced by the rotating bacteria. If the advective water flow was started again after 80 s, the bacteria retreated toward the veil surface by decreasing their stalk lengths. Within 2 min, they returned to their old position close to the veil surface (Fig. 5D) ($t = 80$ to 200 s).

If a 10- by 10-mm piece was removed in the middle of a veil, the resulting hole was subsequently closed by a newly forming veil, which grew at a rate of 2.5 mm h^{-1} from the upstream rim (relative to the flow direction) of the hole. The veil regained its integrity within 4 h.

Microsensor measurements of veils in the enrichment culture showed that the veils were always positioned at the oxic-anoxic interface. The advective water flow parallel to the upper veil surface showed diffusive boundary layers (DBL) between 0.3 and 0.6 mm thick. The oxygen concentration decreased within the boundary layer from air saturation (260 μM O_2) to <2 μM O_2 at the veil surface (data not shown). The sediment surface generally showed high sulfide levels of >1 mM H_2S, which escaped into the overlying water.

Enrichment of veil-forming bacteria in a benthic gradient chamber. We succeeded in culturing the veils in a benthic gradient chamber filled with sulfidic complex medium (Fig. 2). Samples of the veils from the enrichment culture were transferred to the washed sand in the benthic gradient chamber. After 2 to 3 days, several small whitish translucent veils (typically 20 by 20 mm in size) were observed on the sand surface. Successively, new veils developed in the following days on top of older ones. Under homogeneous and laminar flow conditions over the gradient chamber, a single veil finally formed after a week at the upper edge of the beaker, spanning the whole opening (Fig. 2). The whitish translucent veil did not show any structural heterogeneity. No ciliates were observed on its surface. After two more days, the veil became brighter and thicker (~100 μm thick), and it showed perforations of regularly spaced holes ~0.3 mm in diameter (Fig. 7A). In situ video microscopy confirmed that the rotating bacteria were attached to the rims of the holes. Microsensor measurements showed that the veil was positioned at the interface of opposing oxygen-sulfide gradients (Fig. 6B). The oxygen concentration in the DBL decreased within 0.4 mm to <2 μM O_2 on the veil surface. At this stage, only a few ciliates were grazing on the veil (Fig. 7A), whereas a dense ciliate population could be observed on the edge of the benthic gradient chamber at the outer border of the veil (Fig. 7B). Oxygen levels within the ciliate population were typically 10 μM O_2.

Within the following 2 days, the veil surface was completely populated by grazing ciliates with a density of 312 ± 35 cells mm^{-2} (mean ± standard deviation) (Fig. 7C). After three more days, the ciliate population declined to 76 ± 17 cells mm^{-2} (mean ± standard deviation), while the veil surface was now dominated by regularly spaced clusters of *Beggiatoa* filaments (Fig. 7D). Light microscopy of the veil at this stage of development did not show any presence of the rotating bacteria.

We also tried to enrich the veils on noncomplex media. The lower part of the benthic gradient chamber was filled either with medium for purple sulfur bacteria according to Eichler and Pfennig (5) or with medium for marine *Beggiatoa* spp. according Nelson (23). Neutralized Na_2S solution was added to the liquid media to a final concentration of 10 mM. Otherwise, the experimental procedure was as described above for the complex medium. In both cases, we could not observe any veil development within 3 weeks after inoculation.

DISCUSSION

Stalks and veil formation. Attachment by stalks and veil formation are characteristic of the ecology of the new bacteria described in this paper. The stalks were not directly visible by light microscopy, but the threads observed in TEM pictures

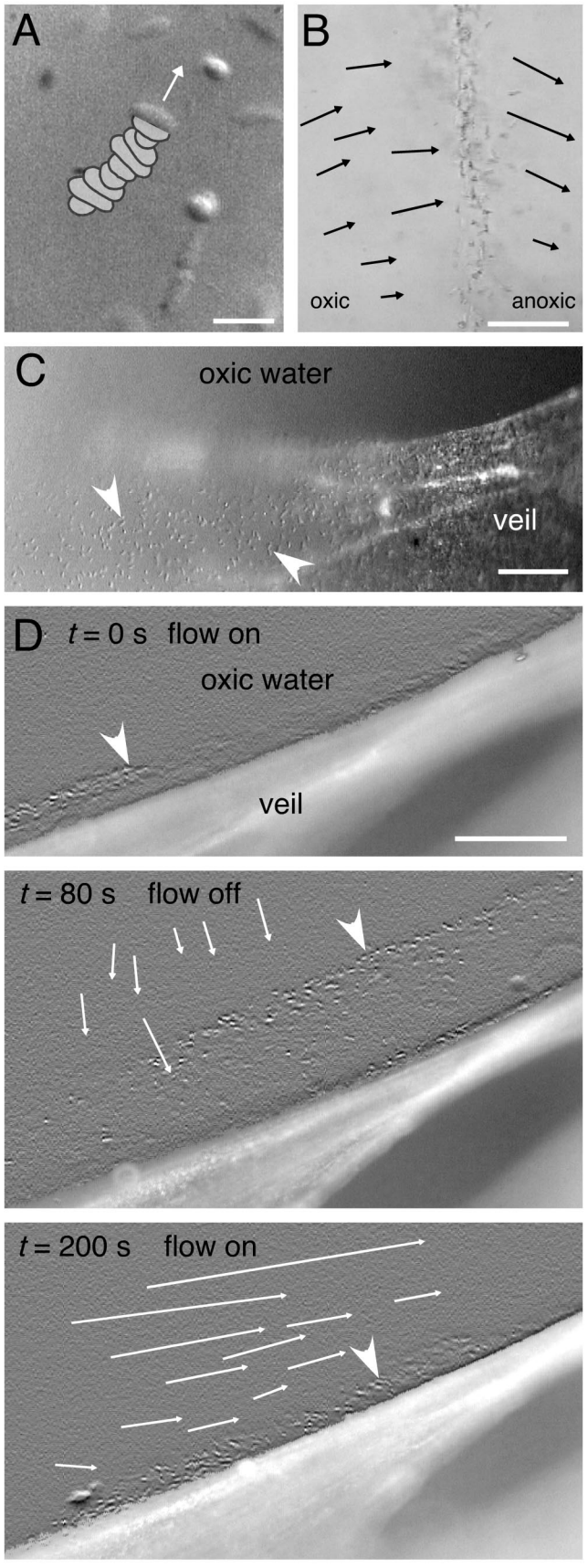

could be remnants of stalks (Fig. 3D). Furthermore, TEM pictures showed protrusions on the cell wall that may be remnants of thin mucous filaments, which are subsequently coiled up to a stalk by the rotational movement of the bacteria. This model implies that the thin filaments have to be constantly excreted in order to keep the stalk length constant. We speculate that the observed fast adjustment of the stalk length could be due to changing excretion rates upon changes in water flow and the local oxygen level of the bacteria. The distribution of the protrusions on the cell surface correlates with the distribution of vesicles just below the cell membrane (Fig. 3F), which may be involved in mucous production.

The formation of elastic mucous webs next to bacterial bands in flat glass capillary preparations revealed the genesis of the whitish translucent veils. Under microoxic conditions (ca. 2 μM O_2), the bacteria continuously excrete a mucous stalk and attach to solid surfaces. Stalks of different bacterial cells successively stick to each other, building up the veil structure. Continuous stalk production would also explain why the thickness of the veils increases over time. The observed fast repair of a hole generated in the veil demonstrates how the veils span depressions or holes in the sediment surface. Veil formation starts on the sediment surface at the upstream side (relative to the prevailing flow direction) of the depression. Chemotactically attracted bacteria probably attach continuously to the downstream edge of the veil. Thus, the veil surface grows until it reaches the opposite side of the depression, where it attaches again to the sediment surface. According to the measured veil growth rate of 2.5 mm h^{-1}, new veils with a typical size of 30 by 30 mm can be generated within 12 h. This agrees well with the observation that new veils were formed de novo within 1 day after the disturbance of the sediment surface in laboratory incubations of sediment.

We observed two mechanisms by which the bacteria position themselves within oxygen gradients at their preferred oxygen concentration of 2 μM O_2. Free-swimming bacteria aggregated chemotactically, whereas attached bacteria adapted their stalk lengths. At steady state, the balance between oxygen consumption by the bacteria and oxygen supply by the advective water flow results in a steep oxygen gradient above the veil, which ensures constant microoxic conditions (2 μM O_2) on the veil

FIG. 5. Motility behavior of the bacteria. (A) Video still image of free-swimming cell. The swimming direction is indicated by an arrow (Normarsky microscopy). The cell's previous positions at consecutive time steps of 0.08 s are superimposed. (B) Bacterial band within a flat glass capillary. The arrows indicate the displacement of tracked neutrally buoyant latex beads within a time interval of 1 s (bright-field microscopy). (C) Rotating bacteria (arrowheads) attached via stalks to whitish translucent veil (in situ video microscopy, contrast enhanced). (D) Rotating bacteria (arrowheads) attached to a whitish translucent veil showing dynamic adaptation of their stalk lengths in response to changing water flow. The stalk lengths were ca. 20 μm at steady state with water flow along the veil surface (t = 0 s). At t = 0 s, the water flow was stopped. The bacteria responded within the next 80 s by prolongation of their stalk lengths, finally exceeding 100 μm (t = 80 s). At t = 80 s, the flow was again started. The bacteria diminished their stalk lengths again and regained their steady-state positions after 2 min (t = 200 s). The thin arrows indicate the displacement of tracked latex beads within a time interval of 1 s (in situ video microscopy, contrast enhanced). Bars, 10 (A), 50 (B), and 100 μm (C and D).

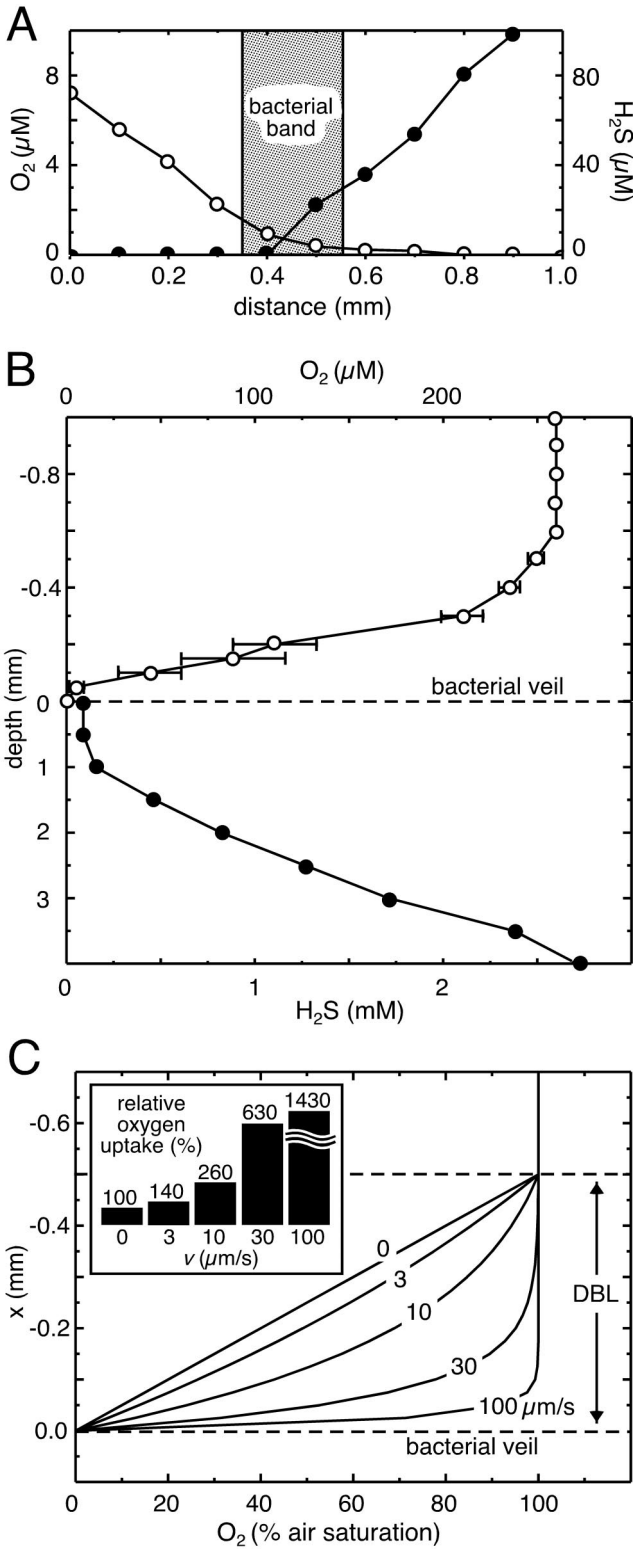

FIG. 6. (A) Oxygen (○) and sulfide (●) gradients across a bacterial band within a flat glass capillary. The shaded region indicates the position of the band. (B) Oxygen (○) and sulfide (●) gradients across a bacterial veil formed on top of benthic gradient chamber. The error bars (where present) indicate the standard deviation ($n = 2$). Note the changing depth scale. (C) Effect of bacterially induced downward water flow on oxygen gradients within the DBL above a whitish translucent veil. Model calculations of oxygen gradients are shown for different downward flow velocities, which are indicated by the adjacent numbers. x represents the distance to the veil. (Inset) Relative oxygen uptake rates at the veil surface calculated for different downward flow velocities (v).

surface. In this case, the bacteria keep constant stalk lengths (Fig. 5C and D) ($t = 0$ s). The position of the oxic-anoxic interface is changed if the steady state is disturbed by changes in the advective water flow, and thus the bacteria can regain their optimal position in the oxygen gradient by shortening or lengthening their stalks (Fig. 5D).

Physiological properties. The bacteria are presumably obligately microaerophilic, preferring an oxygen concentration of 2 μM O_2, because bacteria exposed either to anoxia or to high oxygen concentrations became permanently immotile. The general finding that the veils are positioned at the oxic-anoxic interface within opposing oxygen-sulfide gradients points to a metabolism related to the oxidation of reduced sulfur compounds. However, the present data do not allow positive confirmation of this. The bacteria do not show any sulfur inclusions as in, e.g., the sulfide-oxidizing *Beggiatoa* spp. and *T. majus* (3, 23). Interestingly, the three-layered structure found below the polar cell wall of the bacterium is similar to cell structures observed in bacteria found in filamentous sulfur mats at hydrothermal vents (31). There has been speculation about whether this structure is related to the excretion of solid sulfur filaments observed by light microscopy. Such filamentous-sulfur generation was not observed in our case, although the white color of older veils may be due to the precipitation of elemental sulfur.

Gottschal and Kuenen (12) investigated the influence of the ratio of inorganic (i.e., reduced sulfur compounds) to organic substrates on enrichment cultures for colorless sulfur bacteria. It was found that this ratio was one of the most important environmental parameters affecting the selection of different physiological types of bacteria. When both inorganic and organic compounds were abundant in comparable molar amounts, mixotrophic or chemolithoheterotrophic bacteria became the dominant species in the enrichment culture (28). The same environmental conditions existed in our sediment enrichment cultures, which contained either sediment mixed with decaying algae or sediment inhabited by *Z. marina*. Decaying algae were shown to release considerable amounts of dissolved organic matter (26), whereas the roots of seagrasses were shown to excrete organic compounds (22). Additionally, the measured concentration of >1 mM H_2S on the sediment surface indicates the presence of large amounts of diverse reduced sulfur compounds. Thus, according to the findings of Gottschal and Kuenen (12), the rotating bacteria may be either mixotrophic or chemolithoheterotrophic. However, the picture may be more complicated, as the rotating bacteria were frequently accompanied by other free-swimming spirilla or cocci. One might even speculate about some syntrophic relationship among the different species, as was reported for "*Thiodendron*" mats (4).

Enhanced oxygen uptake. The oxygen uptake rate of anoxic surfaces overlaid by oxic water is generally limited by the diffusive oxygen transport across a thin water layer above the surface, where diffusive transport is predominant (15). The

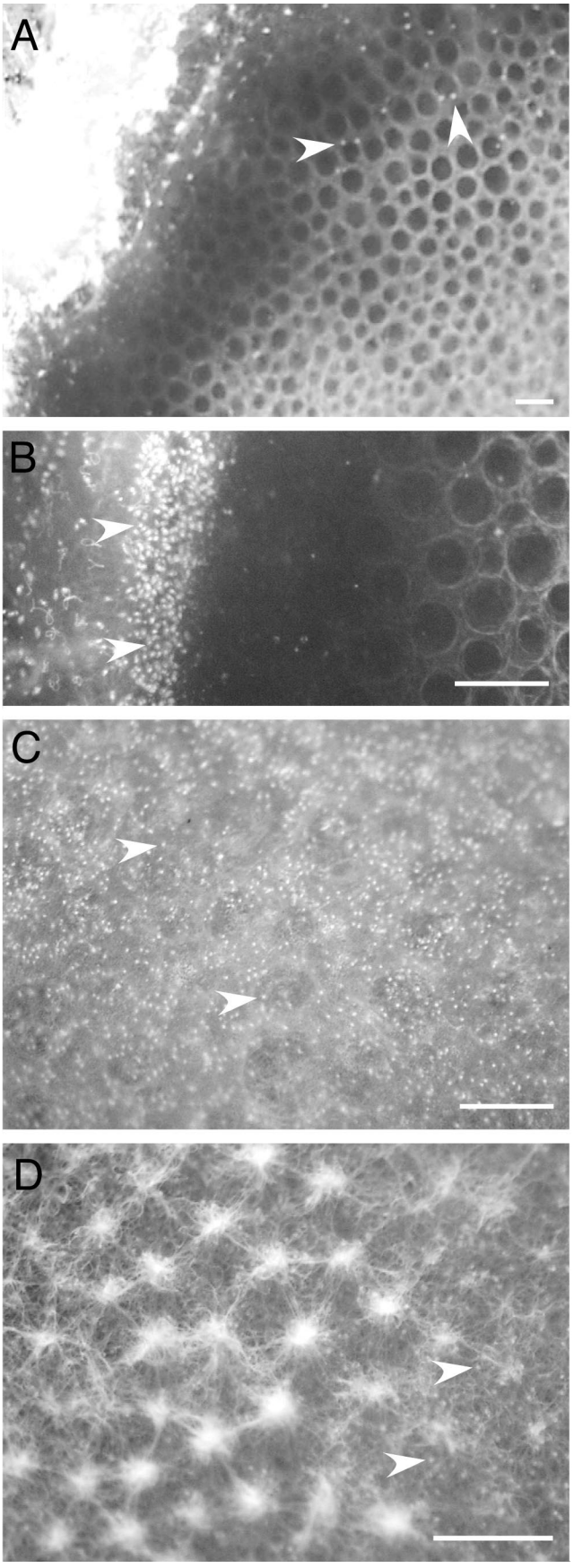

thickness of this so-called DBL is dependent on the flow velocity of the overlying water. We observed that rotating bacteria attached to the veils induced an additional downward water flow. Thus, the oxygen transport within the DBL above the whitish translucent veils is governed by one-dimensional diffusion with a superimposed drift, which at steady state can be described by Fick's second law supplemented with a drift term (1), $D(d^2C/dx^2) - v(dC/dx) = 0$, where D is the free solution diffusion coefficient of oxygen in water, C is the concentration of dissolved oxygen, x gives the distance to the surface (negative values represent positions above the surface), and v is the drift velocity of the induced water flow. This differential equation can be solved analytically, assuming idealized boundary conditions (see the appendix). The resulting oxygen profiles for different drift velocities are shown in Fig. 6C, assuming a typical DBL thickness of 0.5 mm (15) and 100% air saturation (ca. 260 μM O_2) above the DBL and 0% at the veil surface. No drift ($v = 0$ μm s^{-1}) results in a linear oxygen gradient within the DBL, whereas with drift, oxygen profiles obtain an exponential shape.

The oxygen uptake rate, J_o, of the veil is given by the slope of the oxygen profile close to the anoxic veil surface (see the appendix) as follows: $J_o = -D(dC/dx)$ (at $x = 0$). We calculated uptake rates for different drift velocities and related it to the oxygen uptake rate with no drift present (Fig. 6C, inset). In the experiments, we observed drift velocities of ca. 30 μm s^{-1} above the whitish translucent veils, which would correspond to a >6-fold increase in the oxygen uptake rate.

This model for calculating enhanced oxygen uptake by induced downward water flow applies only to freshly developed veils, where the rotating bacteria are evenly distributed on the veil surface. In this case, the necessary countercurrent (i.e., upward water flow) occurs in regions of the sediment surface not covered by veils. Taking into account the typical size of the veils, the rotating bacteria appear to induce a water flow along distances that are >4 orders of magnitude greater than the cell size. The striking structural transformation from a homogeneous veil to a pattern of regularly spaced holes (Fig. 7A) might be caused by the constantly growing veil thickness. The "large-scale" water flow is increasingly inhibited by the thickening veil and is finally replaced by local countercurrents. Regions on the veil with upwelling water currents become anoxic and are consequently abandoned by the microaerophilic bacteria. This process finally results in a veil pattern in which the bacteria are positioned on the rims of holes, inducing a downward water flow, whereas the upward countercurrent flows through the holes next to them.

Similar behavior has been reported for veils formed by the sulfur oxidizer *T. majus.* The bacteria within the veils induced local countercurrents, enhancing the oxygen uptake rate (10).

FIG. 7. Successional pattern of a whitish translucent veil formed on top of a benthic gradient chamber (see Fig. 1). The arrowheads indicate benthic ciliates. (A) Two-day-old veil showing honeycomb pattern of regularly spaced holes. Only a few ciliates are seen on the veil. (B) Detail of a 2-day-old veil (near the right side) showing a dense ciliate population next to the veil border. (C) Four-day-old veil showing a dense ciliate population on its surface. (D) Eight-day-old veil with regularly spaced tufts of *Beggiatoa* spp. Bars, 0.5 mm.

Free-swimming *Thiovulum* cells show velocities up to 600 μm s^{-1} (7). Thus, their flagella produce significantly more kinetic power than the new veil-forming bacteria with swimming velocities of ca. 75 μm s^{-1}. Consequently, attached *Thiovulum* cells should be able to induce higher flow velocities by the action of their flagella. In fact, the oxygen uptake rate of *Thiovulum* veils was estimated to be increased up to 40 times (10).

Ecological strategy. The ecological strategy of the rotating bacteria seems to be opportunistic. During periods of increased wave action, sediment becomes mixed with decaying algae, from which anaerobic microbial processes release large amounts of reduced sulfur as well as reduced organic compounds and nutrients into the overlying oxic water. Aerobic microorganisms recolonize the sediment surface and compete for the reduced substrates. Within 1 day, the rotating bacteria build up their veils above the sediment, stabilizing the oxic-anoxic interface and providing them with their preferred microenvironment. The low oxygen concentration of <2 μM O_2 on the veil surface keeps away other microaerophilic competitors and predators, which generally prefer higher oxygen concentrations. The sulfide oxidizer *T. majus* was shown to prefer oxygen concentrations of 10 μM O_2 (7). Thus, *Thiovulum* has to build its own veil positioned at higher oxygen concentrations above the whitish translucent veils, as was occasionally observed.

Microsensor studies of chemotactic responses of microaerophilic ciliates within oxygen gradients have been performed (8). The ciliates were sampled from the same sulfuretum where the whitish translucent veils were found. Two species showed preferred oxygen concentrations as low as 2.6 μM O_2, whereas four other species showed preferred values from 5 to 50 μM O_2. These findings explain the sharp borderline of a ciliate population positioned at the edge of a veil (Fig. 7B), where oxygen concentrations of ca. 10 μM O_2 were measured. Their chemotactic response prevented them from entering the veil surface at a prevailing oxygen concentration of <2 μM O_2. Taken together, these data explain the observation that no *Thiovulum* spp. and only few grazing ciliates were observed on freshly developed whitish translucent veils.

Species succession. The observed species succession on older veils can also be explained in terms of the oxygen concentration on the veil surface. Veils several days old were covered by a dense ciliate population, indicating that the oxygen concentration on the veil surface had increased. The ciliates grazed heavily on the population of rotating bacteria. At this stage, the veil surface with the increased oxygen level offered ideal conditions for filamentous *Beggiatoa* spp., which are only rarely grazed by ciliates (2). The *Beggiatoa* filaments glided onto and stabilized the anoxic-oxic interface at the position of the old veils by forming a biofilm. The low light attenuation by the thin *Beggiatoa* biofilm provided ideal growth conditions within the anoxic zone below the veil for green and purple sulfur bacteria. Thus, the veil-forming bacteria initialize a unique microbial-mat development above the sediment surface.

A similar species succession has been reported by Bernard and Fenchel (2) for mats of colorless sulfur bacteria. The mats were dominated by *Thiospira* spp. immediately after the samples were brought to the laboratory. After 3 days, the *Thiospira* population disappeared and *Thiovulum* spp. became the dominant species. Finally, after ~1 week, the mat was dominated by *Beggiatoa* spp.

Conclusion and outlook. Bacterial species which are physiologically related to the sulfur cycle have been known for a long time to possess a diversity of unique ecological strategies (20, 30). This report adds a new species to this group of conspicuous bacteria. In situ video microscopy proved to be a powerful tool to unravel the behavior of the bacteria, which in many respects is similar to the behavior of the sulfur-oxidizing bacterium *T. majus.* Future phylogenetic studies will show whether this similarity is due to convergent or divergent evolution.

The physiological properties of the new species have to be determined and investigated in detail. This will require enrichment under more selective conditions yet to be identified. An attempt to isolate the new species in pure culture imposes several difficulties, as besides the presence of opposing oxygen-sulfide gradients, the bacteria also require a moderate water flow above their veils. Furthermore, the ecological relevance and biogeography of the new species are not yet known. Their presence at two different locations indicates that the bacterium may be present in other marine locations that exhibit similar environmental conditions, that is, in coastal sulfidic sediments with a high load of organics.

ACKNOWLEDGMENTS

This study was supported by grants from the European Commission (MAS3-CT98-5054 and EVK3-CT-1999-00010) and the Danish Natural Science Research Council (contract 9700549).

Tom Fenchel, Andrea Wieland, and Alexey Smirnov assisted with many fruitful discussions and much technical advice. We thank Birgit Thorell, Ilse Duun, and Mathias Middelboe for assistance with TEM. Birgit Thorell also assisted in photographic work. Finally, Anni Glud is thanked for manufacturing the microsensors.

APPENDIX

The differential equation for one-dimensional diffusion with a superimposed drift at steady state is given as

$$D(d^2C/dx^2) - v(dC/dx) = 0 \quad (1)$$

where D is the free solution diffusion coefficient of oxygen, C is the oxygen concentration dependent on the distance x, and v is the drift velocity of the induced water flow. This differential equation can be solved by applying the ansatz

$$dC/dx = K_1 \exp(K_2 x) \quad (2)$$

where K_1 and K_2 are free parameters. By substituting equation 2 into equation 1, the parameter K_2 is determined as $K_2 = vD^{-1}$. Integration of equation 2 finally gives

$$C(x) = K_1 \exp(vD^{-1}x) - K_3 \quad (3)$$

with a new free parameter, K_3. The parameters K_1 and K_3 can be determined by applying the boundary conditions $C(-h) = 100\%$ air saturation (a.s.) and $C(0) = 0\%$ a.s., (where h represents the thickness of the DBL) as follows:

$$K_1 = K_3 = 100\% \text{ a.s. } [\exp(-vD^{-1}h) - 1]^{-1} \quad (4)$$

The flux J at any position x of the oxygen profile is given by equation 1

$$J(x) = -D(dC/dx) + vC \quad (5)$$

For $x = 0$, the last term on the right side of equation 5 equals zero; thus, the oxygen uptake rate J_O at the veil surface is given as

$$J_0 = J(0) = -D(dC/dx) \text{ (at } x = 0) \quad (6)$$

REFERENCES

1. **Berg, H. C.** 1993. Random walks in biology. Princeton University Press, Princeton, N.J.
2. **Bernard, C., and T. Fenchel.** 1995. Mats of colourless sulphur bacteria. II. Structure, composition of biota and successional patterns. Mar. Ecol. Prog. Ser. **128:**171–179.
3. **De Boer, W. E., J. W. M. La Rivière, and A. L. Houwink.** 1961. Observations on the morphology of *Thiovulum majus* Hinze. Antonie Leeuwenhoek **27:** 447–456.
4. **Dubinina, G. A., N. V. Leshcheva, and M. Y. Grabovich.** 1993. The colorless sulfur bacterium *Thiodendron* is actually a symbiotic association of spirochetes and sulfidogens. Microbiology **62:**432–444.
5. **Eichler, B., and N. Pfennig.** 1988. A new purple sulfur bacterium from stratified freshwater lakes. Amoebobacter pedioformis sp. nov. Arch. Microbiol. **149:**395–400.
6. **Fenchel, T.** 1969. The ecology of marine microbenthos. IV. Structure and function of the benthic ecosystem, its chemical and physical factors and the microfauna communities with special reference to the ciliated protozoa. Ophelia **6:**1–182.
7. **Fenchel, T.** 1994. Motility and chemosensory behaviour of the sulphur bacterium *Thiovulum majus*. Microbiology **140:**3109–3116.
8. **Fenchel, T., and C. Bernard.** 1996. Behavioural responses in oxygen gradients of ciliates from microbial mats. Eur. J. Protistol. **32:**55–63.
9. **Fenchel, T., and C. Bernard.** 1995. Mats of colourless sulphur bacteria. I. Major microbial processes. Mar. Ecol. Prog. Ser. **128:**161–170.
10. **Fenchel, T., and R. N. Glud.** 1998. Veil architecture in a sulphide-oxidizing bacterium enhances countercurrent flux. Nature **394:**367–369.
11. **Fonselius, S. H.** 1983. Determination of hydrogen sulphide, p. 73–80. *In* K. Grasshoff, M. Ehrhardt, and K. Kremling (ed.), Methods in sea water analysis. Verlag Chemie, Weinheim, Germany.
12. **Gottschal, G. C., and J. G. Kuenen.** 1980. Selective enrichment of facultatively chemolithotrophic *Thiobacilli* and related organisms in continuous culture. FEMS Microbiol. Lett. **7:**241–247.
13. **Jørgensen, B. B.** 1982. Ecology of the bacteria of the sulphur cycle with special reference to anoxic-oxic interface environments. Phil. Trans. R. Soc. Lond. B **298:**543–561.
14. **Jørgensen, B. B.** 1988. Ecology of the sulphur cycle: oxidative pathways in sediments, p. 31–63. *In* J. A. Coles and S. J. Ferguson (ed.), The nitrogen and sulfur cycles. Cambridge University Press, Cambridge, United Kingdom.
15. **Jørgensen, B. B.** 2001. Life in the diffusive boundary layer, p. 348–373. *In* B. P. Boudreau and B. B. Jørgensen (ed.), The benthic boundary layer. Oxford University Press, New York, N.Y.
16. **Jørgensen, B. B., and V. A. Gallardo.** 1999. *Thioploca* spp.: filamentous sulfur bacteria with nitrate vacuoles. FEMS Microbiol. Ecol. **28:**301–313.
17. **Jørgensen, B. B., and N. P. Revsbech.** 1983. Colorless sulfur bacteria, *Beggiatoa* spp. and *Thiovulum* spp., in O_2 and H_2S microgradients. Appl. Environ. Microbiol. **45:**1261–1270.
18. **Kuenen, J. G., L. A. Robertson, and O. H. Tuovinen.** 1992. The genera *Thiobacillus, Thiomicrospira,* and *Thiosphaera*, p. 2638–2657. *In* A. Balows, H. G. Trüper, M. Dworkin, W. Harder, and K.-H. Schleifer (ed.), The prokaryotes, vol. 3. Springer, New York, N.Y.
19. **Kühl, M., C. Steuckart, G. Eickert, and P. Jeroschewski.** 1998. A H_2S microsensor for profiling biofilms and sediments: application in an acidic lake sediment. Aquat. Microb. Ecol. **15:**201–209.
20. **La Rivière, J. W. M., and K. Schmidt.** 1992. Morphologically conspicuous sulfur-oxidizing eubacteria, p. 3934–3947. *In* A. Balows, H. G. Trüper, M. Dworkin, W. Harder, and K.-H. Schleifer (ed.), The prokaryotes, vol. 4. Springer, New York, N.Y.
21. **Møller, M. M., L. P. Nielsen, and B. B. Jørgensen.** 1985. Oxygen responses and mat formation by *Beggiatoa* spp. Appl. Environ. Microbiol. **50:**373–382.
22. **Moriarty, D. J. W., R. L. Iverson, and P. C. Pollard.** 1986. Exudation of organic carbon by seagrass *Halodule wrightii* Aschers and its effect on bacterial growth in the sediment. J. Exp. Mar. Biol. Ecol. **96:**115–126.
23. **Nelson, D. C.** 1992. The genus *Beggiatoa*, p. 3171–3180. *In* A. Balows, H. G. Trüper, M. Dworkin, W. Harder, and K.-H. Schleifer (ed.), The prokaryotes, vol. 4. Springer, New York, N.Y.
24. **Nelson, D. C., and H. W. Jannasch.** 1983. Chemoautotrophic growth of a marine *Beggiatoa* in sulfide-gradient cultures. Arch. Microbiol. **136:**262–269.
25. **Nelson, D. C., N. P. Revsbech, and B. B. Jørgensen.** 1986. Microoxic-anoxic niche of *Beggiatoa* spp.: microelectrode survey of marine and freshwater strains. Appl. Environ. Microbiol. **52:**161–168.
26. **Pedersen, A.-G. U., J. Berntsen, and B. A. Lomstein.** 1999. The effect of eelgrass decomposition on sediment carbon and nitrogen cycling: a controlled laboratory experiment. Limnol. Oceanogr. **44:**1978–1992.
27. **Revsbech, N. P.** 1989. An oxygen microelectrode with guard cathode. Limnol. Oceanogr. **34:**474–478.
28. **Robertson, L. A., and J. G. Kuenen.** 1992. The colorless sulfur bacteria, p. 385–413. *In* A. Balows, H. G. Trüper, M. Dworkin, W. Harder, and K.-H. Schleifer (ed.), The prokaryotes, vol. 1. Springer, New York, N.Y.
29. **Schulz, H. N., T. Brinkhoff, T. G. Ferdelman, M. H. Marine, A. Teske, and B. B. Jørgensen.** 1999. Dense populations of a giant sulfur bacterium in Namibian shelf sediments. Science **284:**493–495.
30. **Schulz, H. N., and B. B. Jørgensen.** 2001. Big bacteria. Annu. Rev. Microbiol. **55:**105–137.
31. **Taylor, C. D., and C. O. Wirsen.** 1997. Microbiology and ecology of filamentous sulfur formation. Science **277:**1483–1485.
32. **Thar, R., and T. Fenchel.** 2001. True chemotaxis in oxygen gradients of the sulfur-oxidizing bacterium *Thiovulum majus*. Appl. Environ. Microbiol. **67:** 3299–3303.
33. **Thar, R., and M. Kühl.** 2001. Motility of *Marichromatium gracile* in response to light, oxygen, and sulfide. Appl. Environ. Microbiol. **67:**5410–5419.